ARCHIVOS DE BRONCONEUMOLOGIA

Original Article

Development of a Murine Model of Airway Inflammation and Remodeling in Experimental Asthma

Rebeca Fraga-Iriso, Laura Núñez-Naveira, Nadia S. Brienza, Alberto Centeno-Cortés, Eduardo López-Peláez, Héctor Verea, and David Ramos-Barbón*

Unidad de Investigación Respiratoria, Servicio de Neumología, Complejo Hospitalario Universitario, Instituto de Investigación Biomédica de A Coruña (INIBIC), A Coruña, Spain

ABSTRACT

Background and Objective: Experimental animal models are necessary for studying asthma disease mechanisms and for identifying new therapeutic targets. We present a murine model of experimental asthma that allows integrated, quantitative assessment of airway inflammation and remodeling.
Material and Methods: BALB/c mice were sensitized to ovalbumin (OVA) and challenged with OVA or vehicle 3 times per week for 12 weeks.
Results: On bronchoalveolar lavage, the OVA-sensitized mice had significantly higher total leukocyte counts, with a median (Q25-Q75) of 670.0 cells/mL×10^{-3} (376.2-952.5) in comparison with 40.0 cells/mL×10^{-3} (60.0-85.0) in controls (*P*=.001), and higher eosinophil and differential lymphocyte counts. In sagittal sections of lungs inflated to a standard pressure, the OVA-sensitized animals showed goblet cell hyperplasia in the respiratory epithelium (periodic acid-Schiff staining, 53.89 [36.26-62.84] cells/mm² vs 0.66 [0.00-1.06] cells/mm², *P*<.001), dense mononuclear and eosinophilic inflammatory infiltrates (hematoxylin-eosin, 32.87 [27.34-37.13] eosinophils/mm² vs 0.06 [0.00-0.20] eosinophils/mm², *P*=.002), subepithelial infiltration by mast cells (toluidine blue, 2.88 [2.00-3.28] mast cells/mm² vs 0.28 [0.15-0.35] mast cells/mm², *P*<.001), increased contractile tissue mass (immunofluorescence analysis for α-smooth-muscle actin, 2.60 [2.28-2.98] vs 1.08 [0.93-1.16], dimensionless, *P*<.001) and enhanced extracellular matrix deposition (Masson's trichrome, 2.18 [1.85-2.80] vs 0.50 [0.37-0.65], dimensionless, *P*<.001).
Conclusions. Our dataset describes an experimental model of asthma which is driven by prolonged allergen exposure and in which airway inflammation and remodeling develop and are assessed together.

© 2008 SEPAR. Published by Elsevier España, S.L. All rights reserved.

Desarrollo de un modelo murino de inflamación y remodelación de vías respiratorias en asma experimental

RESUMEN

Introducción: La investigación de los mecanismos de enfermedad del asma y la identificación de nuevas dianas terapéuticas requieren modelos animales experimentales. En este trabajo presentamos los datos del desarrollo de un modelo murino de asma experimental que permite valorar de forma conjunta parámetros de inflamación y remodelación de las vías respiratorias mediante morfología cuantitativa.
Material y métodos: Se sensibilizó a ovoalbúmina a ratones Balb/c y se les realizó broncoprovocación con ovoalbúmina o excipiente 3 veces por semana durante 12 semanas.
Resultados: En el lavado broncoalveolar, los ratones del grupo de ovoalbúmina presentaron un incremento significativo de leucocitos totales, con una mediana (cuartiles 25–75) de 670,0 células/ml·10^3 (376,2–952,5), frente a 40,0 células/ml·10^3 (60,0–85,0) en controles (p = 0,001), y de las fracciones eosinófila y linfocitaria en recuento diferencial. En secciones sagitales de los pulmones inflados a presión estandarizada, estos ra-

*Corresponding author.
E-mail address:* David.Ramos.Barbon@sergas.es (D. Ramos-Barbón).

tones mostraron hiperplasia de células caliciformes en el epitelio respiratorio —reacción de ácido peryódico de Schiff: 53,89 (36,26–62,84) frente a 0,66 (0,00–1,06) células/mm² (p < 0,001)—, densa infiltración inflamatoria mononuclear y eosinófila —hematoxilina-eosina: 32,87 (27,34–37,13) frente a 0,06 (0,00–0,20) eosinófilos/mm² (p = 0,002)—, infiltración subepitelial por mastocitos —azul de toluidina: 2,88 (2,00–3,28) frente a 0,28 (0,15–0,35) mastocitos/mm² (p < 0,001)—, incremento de la masa de tejido contráctil —inmunofluorescencia para alfaactina de músculo liso: 2,60 (2,28–2,98) frente a 1,08 (0,93–1,16), adimensional (p<0,001)— e incremento del depósito de matriz extracelular (tricrómico de Masson: 2,18 (1,85–2,80) frente a 0,50 (0,37–0,65), adimensional (p < 0,001)—.

Conclusiones: Los datos aportados configuran un modelo de asma experimental inducida por exposición alergénica prolongada, con desarrollo y evaluación integrada de inflamación y remodelación de vías respiratorias.

Introduction

Asthma is unanimously considered to be a growing problem due to its sustained increase in recent decades, its morbidity and mortality, and the economic burden that it involves.[1] Despite the treatments that are currently available, a high proportion of asthma cases are still severe and difficult to manage. Many research efforts are therefore aimed at improving our understanding of its pathogenic mechanisms and identifying therapeutic or preventive targets that offer new strategies for managing the disease.[2]

Animal models are an essential resource for adding to our knowledge of disease mechanisms and a key element in bridging the gap between basic research and clinical practice. The knowledge provided by these models leads to new therapeutic approaches that are in turn applied again in animal models of disease in their preclinical stage of development. In asthma, most animal model datasets have been obtained in the mouse and the rat, each of which has advantages and limitations.[3-5] The design of the experimental protocols varies greatly and the aspects of the disease to be studied may differ in each case. In the case of mice, this species versatility has made it possible to generate transgenic animals, but in general the effect of the genetic modifications has been studied without inducing the immune responses that would establish a basis for a model of disease.[4] Despite the technology available, few studies present quantitative assessments of airway inflammation and remodelling together. In this paper we present the dataset obtained from our laboratory's creation of a murine model of experimental asthma based on repeated long-term antigen exposure, with development and quantitative assessment of airway inflammation and remodeling. This general model of severe chronic disease can be transferred to the investigation of specific objectives in future studies and adapted to the use of transgenic strains.

Material and Methods

Animals, Sensitization, Challenge and Processing of the Lungs

The experimental design is summarized in Figure 1. On days 0 and 7 of each experiment female BALB/c mice (Harlan Interfauna Ibérica, SL, Sant Feliu de Codines, Barcelona, Spain) were sensitized by intraperitoneal injection of 10 μg of ovalbumin (Grade IV, Sigma-Aldrich, Madrid, Spain) dissolved in a suspension of aluminum hydroxide (Pierce Immunochemicals, Cultek SLU, Madrid, Spain) in phosphate-buffered saline (PBS). From day 14 the mice were subjected to bronchial challenge by intranasal instillation of 100 μg of ovalbumin diluted in PBS (OVA group, n=8) or PBS (control group, n=8). Under light anesthesia with sevoflurane (Sevorane, Abott Laboratories SA, Madrid, Spain), 25 μl of solution was administered in each nostril 3 times per week for 12 weeks. The mice received deep anesthesia with sevoflurane 48 hours after the last bronchial challenge so that they could undergo tracheostomy and insertion of a 20-caliber flexible propylene Fisnar tube (Dotest SL, Barcelona, Spain). Bronchoalveolar lavage was performed with 5 mL of PBS in fractions of 1 mL and the cellular fraction was separated for total leukocyte counts in a hemocytometer and differential leukocyte counts in cytocentrifuged samples fixed in methanol and stained with Wright-Giemsa stain.
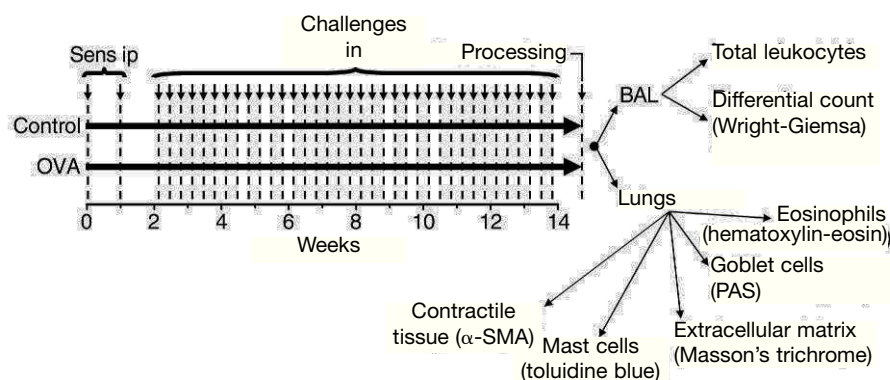
Figure 1. Diagram of the experimental design. The mice were sensitized intraperitoneally (Sens ip) with ovalbumin (OVA) on days 0 and 7. From day 14 they were subjected to an intranasally (in) administered bronchial challenge with vehicle (control group) or OVA 3 times per week for 12 weeks. Bronchoalveolar lavage (BAL) was performed 48 hours after the last challenge for the total and differential leukocyte counts and the lungs were fixed by filling to a standard pressure. Lung sections were processed for different measurements, as indicated, and quantitative morphology was carried out. α-SMA indicates α-smooth-muscle actin detected by immunofluorescence; PAS, periodic acid-Schiff reaction.

After collection of the bronchoalveolar lavage fluid, the pulmonary vascular circuit was perfused through the right ventricle with edetic acid (2 mM in PBS) and the cardiopulmonary block was then removed. The lungs were fixed by filling them through the tracheal cannula with 4% formaldehyde at a standard pressure of 25 cmH_2O, which was maintained for 24 hours by means of a pump and a recirculation system. The lungs were divided into hilar and peripheral parts by section in the sagittal plane and embedded in paraffin for later analysis. The study protocol was approved by the bioethics committee of the government (Xunta) of Galicia as complying with European Union Directive 86/609 and the subsequent Royal Decree 1201/2005 and Order of September 15, 2006.

Histopathologic Examination

Lung sections of 4 μm thickness were stained with hematoxylin-eosin for qualitative histopathological assessment. We also applied the following stains: periodic acid-Schiff staining to detect and count mucus-producing goblet cells; hematoxylin-eosin staining to identify eosinophils; toluidine blue staining for mast cells; and Masson's trichrome staining for the extracellular matrix. The contractile tissue of the airways (smooth muscle and myofibroblasts) was detected by immunofluorescence using an α-smooth-muscle actin monoclonal antibody (α-SMA, clone 1A4, Sigma-Aldrich). For this procedure, the preparations were deparaffinized, permeabilized with 0.2% Triton X-100 (Sigma-Aldrich) and blocked with Image-IT Signal Enhancer (Molecular Probes, Invitrogen, Prat de Llobregat, Barcelona, Spain). A 1A4 antibody was combined with a (Fab')2 anti-mouse IgG2a labeled with Alexa 488 (Zenon, Molecular Probes, Invitrogen) and incubated for 30 minutes on the preparations at a concentration of 2 μg/mL. The samples were then counterstained with 4',6-diamidine-2-phenylindole (DAPI; Molecular Probes, Invitrogen), fixed in 4% paraformaldehyde and mounted with ProLong Gold (Molecular Probes, Invitrogen).

Quantitative Morphology

Airway cross sections from the prepared lungs were analyzed according to sampling and standardization criteria established elsewhere.[6] The mean (SD) number of airways measured per animal was 13.8 (1.4). The cell counts (goblet cells, eosinophils, and mast cells) were standardized by dividing by the square of the perimeter of the basement membrane (P_{BM}^2) of the airway and are expressed as cells per millimeter. P_{BM}^2 was used to correct measurements for airway size because it was considered to be the most constant dimension, regardless of the degree of airway constriction or relaxation.[6] This measure was based on calibrated digital images of the airways, and the perimeter of the basement membrane was traced using a digital tablet in an image analysis program (AnalySIS, Soft Imaging System GmbH, Olympus España SAU, Barcelona, Spain). For the quantitative determination of the extracellular matrix component in the preparations stained with Masson's trichrome, a color extraction algorithm was developed in AnalySIS and the surface of the resulting particles was detected and measured on the airway wall using the same program. In each airway the sum of the particle surface was standardized by dividing by P_{BM}^2; the result was called the "extracellular matrix mass" (M_{EXM}). For the standardized measurement of the contractile tissue, its immunofluorescence signal was digitized, the surface of the resulting particles was detected and measured, and the sum of the surfaces was standardized for P_{BM}^2. Though this parameter has been called "smooth muscle mass", we adopted the proposal of some authors to call it the airway "contractile tissue mass" (M_{CT}) because, in addition to detecting the smooth muscle cells, the antibody 1A1 detects myofibroblasts that express the muscle isoform of α-actin. The parameters M_{EXM} and M_{CT} are dimensionless indices.

Statistical Analysis

The data are expressed as the median, 25th to 75th quartiles and 10th to 90th percentiles. The comparisons between distributions of the control and OVA groups were made using the *t* test for independent samples. To categorize the airways by size as small, medium and large, the values 0.8 mm and 1.5 mm were taken as the cutoffs for the length of the perimeter of the basement membrane. The data were analyzed according to airway size category by analysis of variance (ANOVA) followed by the Fisher least significant difference as a post hoc test. The size of the differential gradient along the airways of different sizes was estimated by the 95% confidence interval of the mean difference (95% CI). Where applicable, the strength of association between variables was assessed by the Pearson correlation coefficient. The statistical significance was set at $P<.05$. The programs SPSS version 15.0 and SigmaPlot version 2000 were used.

Results

Airway Inflammation

The total cell counts in the bronchoalveolar lavage fluid in the OVA group was 10.6 times higher than that in the control group, and the differential leukocyte count showed that the infiltrate was eosinophilic and lymphocytic (Figure 2). OVA group tissue sections contained mononuclear and eosinophilic inflammatory infiltrates, mainly located in the membrane and adventitia of the airway wall and in the bridges of connective tissue between the airways and the
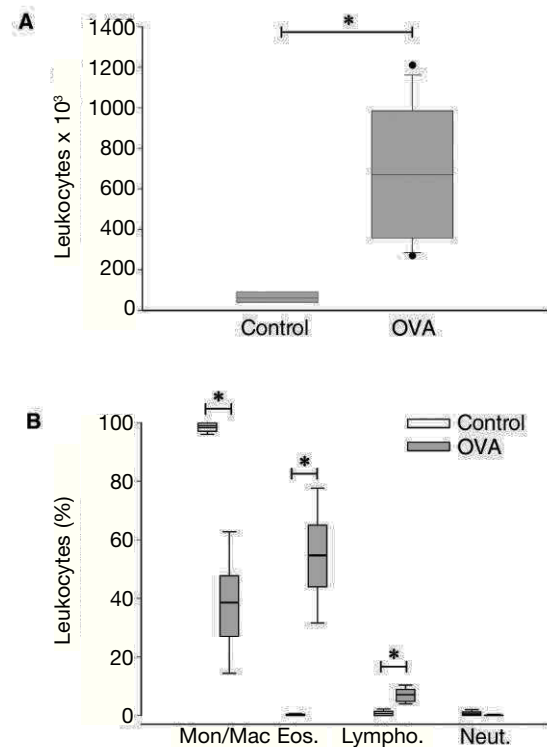

Figure 2. Cell counts in bronchoalveolar lavage fluid. *A*, total leukocyte count in a hemocytometer. *B*, differential cell count based on Wright-Giemsa staining (monocytes/macrophages [mon/mac], eosinophils [eos], lymphocytes [lympho] and neutrophils [neut]). The box plots indicate the median, 25th-75th quartiles (limits of the box) and 10th-90th percentiles (error bars). OVA indicates mice challenged with ovalbumin. *P<.05.

adjacent vessels of pulmonary circulation (Figure 3 A–C). Quantitatively (Figure 4, A–B), mice in the OVA group had higher eosinophil counts in all these locations and more mast cells mainly in a subepithelial location (Figure 3 D).

Structural Remodeling

The structural remodeling of the airways (Figure 3 E–P) was assessed by standardized count of goblet cells positive for the periodic acid-Schiff reaction in the bronchial epithelium and by the M_{CT} and M_{EXM} indices, which reflect, respectively, the smooth muscle and fibrogenic growth components of remodeling. Animals in the OVA group showed goblet cell hyperplasia and a functional state of hypersecretion (Figures 3 E–H and 4 C). OVA group animals also had significantly higher M_{CT} and M_{EXM} indices than the controls (Figures 3 I–P and 5). Under normal conditions (control group), along the bronchial tree we observed a progression towards a slightly higher M_{CT} as airway caliber decreased (95% CI of the increment was −1.14, −0.77; correlation of M_{CT} with P_{BM}, $r=−0.27$, $P=.012$) (Figure 6 A). The M_{CT} in the OVA group was 2.56 times that of the control group overall, and the differences were significant in all airway size categories. The M_{CT} distribution was approximately homogeneous along the bronchial tree ($P=.215$, ANOVA between airway size categories). In the control group the M_{EXM} was significantly greater in the large and
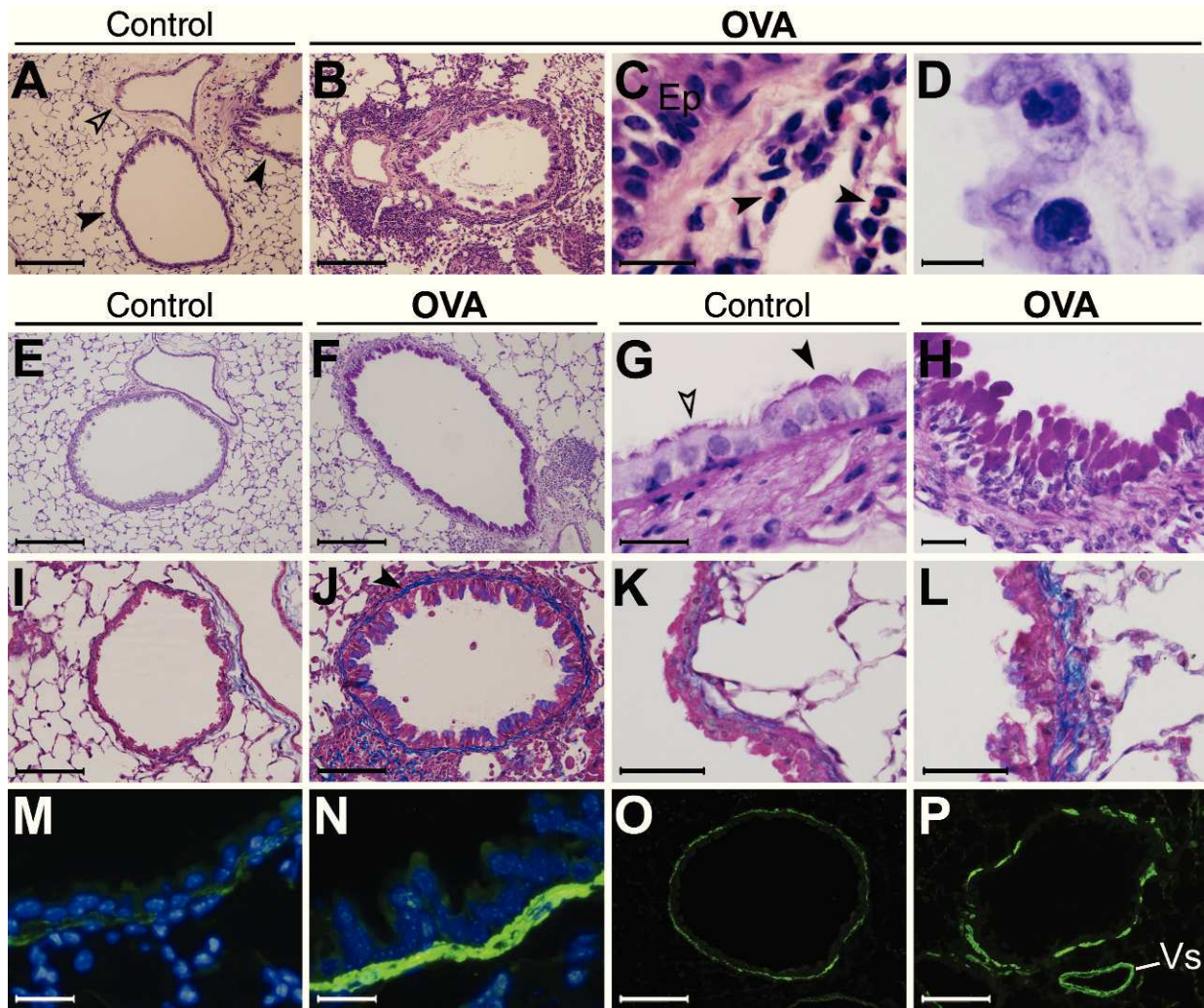
Figure 3. Microscopy. *A–C,* hematoxylin-eosin. *A,* image corresponding to a mouse of the control group, showing the airways (black arrowheads) and an accompanying artery (transparent arrowhead). *B,* airway and nearby vessel in mouse of the OVA group. A dense inflammatory infiltrate can be seen in the airway and the perivascular region. The airway wall is thicker and the lumen contains residues of cell mucus and detritus. *C,* detail showing the mononuclear and eosinophilic inflammatory infiltrates (arrow tips) Ep, respiratory epithelium.
*D,* toluidine blue. Two mast cells very near the respiratory epithelium in an OVA group animal. The characteristic metachromatic granular material can be seen in their cytoplasm.
E–H, periodic acid-Schiff (PAS) reaction. *E* and *F,* respectively, control and OVA animals; in the latter one can see the abundant PAS-positive epithelial content. *G,* detail of the respiratory epithelium of a control animal. The PAS-positive granules of mucus material are concentrated at the apical pole of the goblet cells (black arrow tip). The secreted material forms part of the surface fluid of the airways and can be seen on the ciliated cells (transparent arrowhead). *H,* in OVA animals, one can see goblet cell hyperplasia with an accumulation of PAS-positive material, reflecting a hypersecretory state.
I–L, Masson's trichrome. The fibrous extracellular matrix deposition in the connective tissue is seen in blue. *I,* mouse of the control group, showing normal-density matrix. *J,* mouse of the OVA group, showing subepithelial fibrosis (arrow tip). *K* and *L,* details of mice of the control and OVA groups; in the latter one can see the increased extracellular matrix deposition.
M–P, immunofluorescence for α-smooth-muscle actin (α-SMA; green) and nuclear counterstaining (blue). *M* and *N,* mice of the control and OVA groups, respectively: in the latter one can see the thickening of the smooth-muscle layer. *O* and *P,* extraction of the α-SMA signal for measurement of the contractile tissue mass; mice of the control and OVA groups, respectively. *P,* vascular (Vs) smooth muscle is also visible, but is excluded from the measurements.
Scale bars: 200 μm in A, B, E and F; 100 μm in I, J, O and P; 50 μm in K and L; 25 μm in H, M and N; 20 μm in C and G, and 10 μm in D.
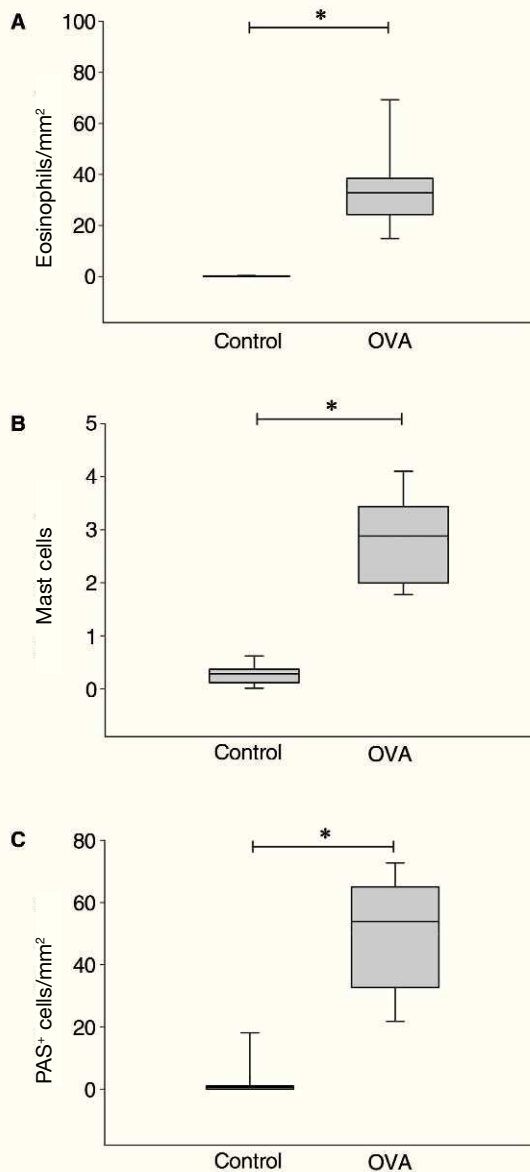
Figure 4. Eosinophils *(A)*, Mast Cells *(B)* and PAS-Positive Goblet Cells *(C)* on the airway walls. Cell counts standardized by dividing by the square of the perimeter of the basement membrane. For each study group, the box plots indicate the median, 25th-75th quartiles (upper and lower edges of the box) and 10th-90th percentiles (error bars). OVA indicates the group challenged with ovalbumin. *$P<.001$.

medium-caliber airways (95% CI of the mean increment between large and small airways, 0.35, 1.02; correlation of M_{EXM} with P_{BM}: $r=0.42$, $P=.002$)(Figure 6 B), indicating that in physiologic conditions the extracellular matrix deposition is higher in larger-caliber airways. The M_{EXM} in the OVA group was 4.16 times greater than in the control group; M_{CT} also increased significantly in all airway size categories and was distributed homogeneously along the bronchial tree ($P=.051$ between airway size categories).

Discussion

Of the species used to create experimental asthma models, the mouse is the most widely used due to its cost-effectiveness and versatility.[5] To develop these models further, we currently need to apply genetic engineering techniques to murine models of human immune response in asthma. Also needed is the integrated analysis of inflammation and remodeling and the components of remodeling, with special attention to the airway smooth muscle. In this paper we have presented the dataset of a murine model integrating inflammation and remodeling through intraperitoneal sensitization to ovalbumin followed by intranasal challenge. The model produced dense mononuclear and eosinophilic inflammatory infiltrates, an increase in the number of mast cells, and remodeling with an increase in the number of mucus-producing goblet cells, subepithelial fibrosis, an increase in the M_{CT}, and an overall increase in the airway wall thickness in all the wall layers.

Ovalbumin is the antigen most often used to induce experimental allergic asthma. However, its systematic use has been criticized because it is not an aeroallergen that produces human disease through inhalation. For this reason, alternative models using allergens such as dust mites[7,8] and pollen[9] have been developed. In the model of Johnson et al,[8] the animals were exposed exclusively to house dust mite extract intranasally for 7 weeks without previous systemic sensitization, closely reflecting the process of sensitization to allergens in humans. However, a special advantage of ovalbumin is the current availability of a strain of transgenic mice (DO11.10) that express the specific T cell receptor for this antigen[10] in all their CD4+ T cells, thus providing a highly useful tool for analyzing the antigen-specific immunological mechanisms of T cells in asthma through adoptive transfer experiments that use the model presented herein. This is the main reason for the use of ovalbumin in our model, despite its limitations.

The protocols of the different models vary according to the hypotheses that are to be tested. A simple bronchial challenge after systemic sensitization may cause inflammation of the airways and, in fact, most models that have been developed have been of short duration and have focused on the inflammatory aspect of the disease. However, the development of remodeling requires a longer exposure, and this aspect has not been dealt with in most models. In several studies prolonged exposure to ovalbumin produced a decline in the inflammatory response in the airways, but the protocols were based on primary exposure through inhalation without previous parenteral sensitization.[11-13] When Emelkovski et al[14] compared prolonged bronchial challenge with ovalbumin with and without previous intraperitoneal sensitization, they observed that primary exposure in the respiratory system produced a decline in the response that coincided with the results of previous studies. However, prolonged bronchial challenge after intraperitoneal sensitization produced sustained inflammation and structural changes. In a similar study, McMillan and Lloyd[15] observed persistent inflammation and remodeling after a protocol of intraperitoneal sensitization and repeated bronchial challenge lasting 55 days in all. This set of studies suggests that primary exposure to ovalbumin in the respiratory system induces immunological tolerance, whereas prolonged bronchial challenge after intraperitoneal sensitization produces allergic disease with persistent inflammation and remodeling. In our study we used intraperitoneal sensitization and established the longest repeated bronchial challenge protocol that we are aware of in order to simulate in the mouse the chronicity of the human disease and to estimate the maximum effects in a severe asthma model. In contrast with the development of tolerance reported after primary exposure to ovalbumin in the respiratory tract, it is interesting that Johnson et al,[8] who used house dust mite extract in this mode, observed the development of inflammation and remodeling in their model. A feature that is lacking in all these models is the integrated study of the allergic response in the upper airway and lungs. Some authors have stressed that it is important to analyze the interrelation and joint evolution of allergic rhinitis and asthma, and have developed their own models for achieving this.[16,17]

Several noteworthy aspects can be observed in our model. The microlocalization of mast cells within the airway smooth muscle of
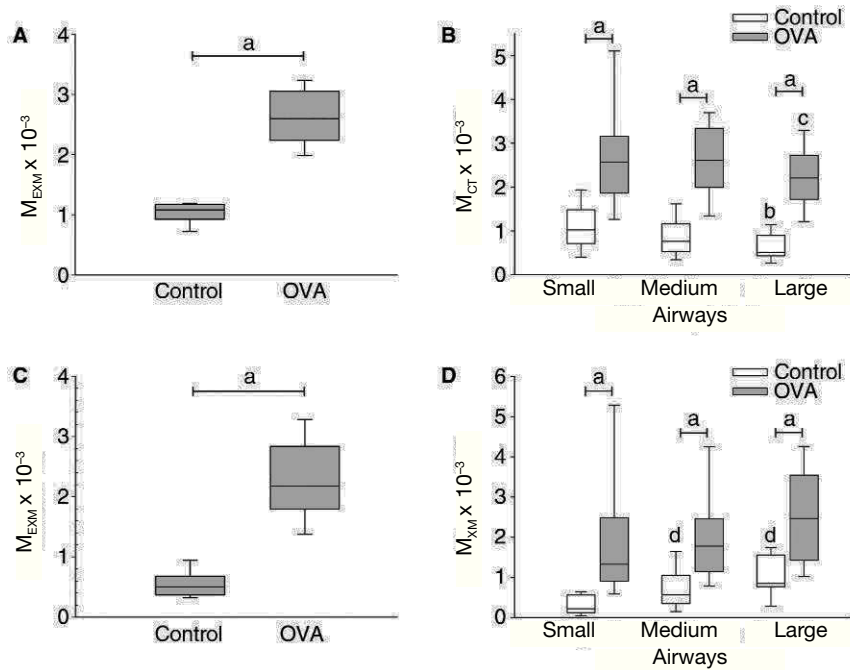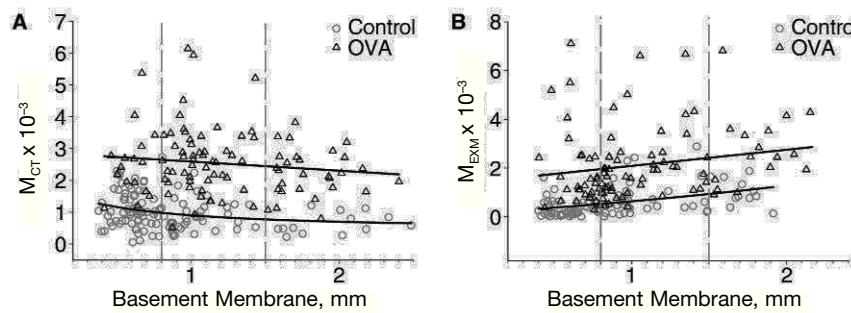
Figure 5. Increase in contractile tissue mass (M_{CT}) and extracellular matrix mass (M_{EXM}) in the airway remodeling. *A* and *C*, M_{CT} and M_{EXM}, respectively, in the study groups. *B* and *D*, distribution of M_{CT} and M_{EXM}, respectively, according to the size category of the airways in each group. The box plots indicate the median, 25th-75th percentiles (limits of the box) and 10th-90th percentiles (error bars). OVA indicates the group challenged with ovalbumin.
[a]$P<.001$.
[b]$P=.005$ compared with the small airways in the control group.
[c]Intermediate difference from small airways in the OVA group.
[d]$P<.001$ compared with small airways in the control group.

Figure 6. Scatterplots of the values of the contractile tissue mass (M_{CT}) (*A*) and extracellular matrix mass (M_{EXM}, *B*) in the airways according to their size, measured by the perimeter of the basement membrane. The vertical dashed lines indicate the cut points of the small, medium and large size airway categories. The regression lines correspond, respectively, to the control (bottom) and OVA-challenged (top) groups in each panel.

patients with asthma has recently been documented[18] and the potential pathophysiologic implications of this finding are considered to be important. In our model mast cells, increased in number, were distributed in the subepithelial region and occasionally within the epithelium or adventitia, but we observed no mast cells within the smooth muscle layer. The absence of this phenomenon should be interpreted with caution, because in the mouse the cell size is proportionally less reduced than the anatomical structures overall. Consequently, the thickness of the airway smooth muscle layer of the mouse may be insufficient to contain mast cells, but the direct action on the muscle of mast cell mediators situated at a short distance is still feasible. Secondly, we consider that goblet cell hyperplasia, which is reported in the literature to be observed

through the use of mucus-detecting stains, may be partly the result of a hyperfunctional state of these cells, which cannot be identified easily in control animals or persons without asthma. A high-magnification examination in the control animals suggests that in their normal state the goblet cells maintain a balanced flow of production and secretion of mucus, so they accumulate very small amounts of mucus in their cytoplasm. In animals with experimental asthma the goblet cells have a cytoplasm that is highly distended and engorged with mucus, which makes them particularly visible. The high number of these hypertrophic cells could indicate that a hyperplastic process is involved, but the contribution of cell proliferation to mucus metaplasia has not yet been quantitatively determined. Finally, with regard to the increase in the M_{CT}, it is worth

noting that this dimensionless index has the same value in mice as in rats[19] and horses,[20] suggesting that the amount of smooth muscle standardized for airway size is constant across species. The magnitude of the increase in the M_{CT} in mice with experimental asthma is also similar to that observed in rats and horses with heaves, an obstructive allergic disease that occurs naturally in these animals. The distribution of the M_{CT} in airways of different sizes remained nearly constant in the controls, as in rats and horses. However, it is noteworthy that the increase in the M_{CT} in the OVA-sensitized mice was distributed homogeneously along the bronchial tree, whereas in the induced disease in a rat model and in heaves in horses, this value grows exponentially towards the peripheral airways. This different behavior may be related to the anatomical—and probably functional—differences between the airway tree of the mouse and that of larger mammals.[4]

In conclusion, the dataset presented here corresponds to the initial development of a model of inflammation and remodeling that will serve as a basis for future studies. The evolution of our conceptual understanding of the pathogenesis of asthma from bronchoconstriction to inflammation and remodeling—together with clinical data that suggest the relevance of managing asthma "in accordance with remodeling" and the need for preclinical development of new "antiremodeling" drugs—calls on us to develop more mature experimental disease models with an immunological basis so that we can assess the quantitative variables of airway inflammation and remodeling together. Such models should serve as a basis for translational research in genetic modification.

Funding

References

1. Masoli M, Fabian D, Holt S, Beasley R. The global burden of asthma: executive summary of the GINA Dissemination Committee report. Allergy. 2004;59:469-78.

2. Ramos-Barbón D. Investigación básica en asma: ¿hacia dónde nos dirigimos? Arch Bronconeumol. 2006;42:613-5.

3. Cortijo J. Modelos experimentales de asma. Aportaciones y limitaciones. Arch Bronconeumol. 2003;39:54-6.

4. Ramos-Barbón D, Ludwig MS, Martin JG. Airway remodeling: lessons from animal models. Clin Rev Allergy Immunol. 2004;27:3-22.

5. Torres R, Picado C, De Mora F. Descubriendo el asma de origen alérgico a través del ratón. Un repaso a la patogenia de los modelos de asma alérgica en el ratón y su similitud con el asma alérgica humana. Arch Bronconeumol. 2005;41:141-52.

6. James AL, Hogg JC, Dunn LA, Pare PD. The use of the internal perimeter to compare airway size and to calculate smooth muscle shortening. Am Rev Respir Dis. 1988;138:136-9.

7. Lambert AL, Winsett DW, Costa DL, Selgrade MK, Gilmour MI. Transfer of allergic airway responses with serum and lymphocytes from rats sensitized to dust mite. Am J Respir Crit Care Med. 1998;157:1991-9.

8. Johnson JR, Wiley RE, Fattouh R, Swirski FK, Gajewska BU, Coyle AJ, et al. Continuous exposure to house dust mite elicits chronic airway inflammation and structural remodeling. Am J Respir Crit Care Med. 2004;169:378-85.

9. Cates EC, Gajewska BU, Goncharova S, Álvarez D, Fattouh R, Coyle AJ, et al. Effect of GM-CSF on immune, inflammatory, and clinical responses in a novel mouse model of mucosal sensitization. J Allergy Clin Immunol. 2003;111:1076-86.

10. Murphy KM, Heimberger AB, Loh DY. Induction by antigen of intrathymic apoptosis of CD4+CD8+TCRlo thymocytes in vivo. Science. 1990;250:1720-3.

11. Holt PG, Batty JE, Turner KJ. Inhibition of specific IgE responses in mice by pre-exposure to inhaled antigen. Immunology. 1981;42:409-17.

12. Sedgwick JD, Holt PG. Down-regulation of immune responses to inhaled antigen: studies on the mechanism of induced suppression. Immunology. 1985;56:635-42.

13. Swirski FK, Sajic D, Robbins CS, Gajewska BU, Jordana M, Stampfli MR. Chronic exposure to innocuous antigen in sensitized mice leads to suppressed airway eosinophilia that is reversed by granulocyte macrophage colony-stimulating factor. J Immunol. 2002;169:3499-506.

14. Temelkovski J, Hogan SP, Shepherd DP, Foster PS, Kumar RK. An improved murine model of asthma: selective airway inflammation, epithelial lesions and increased methacholine responsiveness following chronic exposure to aerosolised allergen. Thorax. 1998;53:849-56.

15. McMillan SJ, Lloyd CM. Prolonged allergen challenge in mice leads to persistent airway remodelling. Clin Exp Allergy. 2004;34:497-507.

16. Hellings PW, Hessel EM, Van Den Oord JJ, Kasran A, Van Hecke P, Ceuppens JL. Eosinophilic rhinitis accompanies the development of lower airway inflammation and hyper-reactivity in sensitized mice exposed to aerosolized allergen. Clin Exp Allergy. 2001;31:782-90.

17. Hellings PW, Ceuppens JL. Mouse models of global airway allergy: what have we learned and what should we do next? Allergy. 2004;59:914-9.

18. Brightling CE, Bradding P, Symon FA, Holgate ST, Wardlaw AJ, Pavord ID. Mast-cell infiltration of airway smooth muscle in asthma. N Engl J Med. 2002;346:1699-705.

19. Ramos-Barbón D, Presley JF, Hamid QA, Fixman ED, Martin JG. Antigen-specific CD4+ T cells drive airway smooth muscle remodeling in experimental asthma. J Clin Invest. 2005;115:1580-9.

20. Herszberg B, Ramos-Barbón D, Tamaoka M, Martin JG, Lavoie JP. Heaves, an asthma-like equine disease, involves airway smooth muscle remodeling. J Allergy Clin Immunol. 2006;118:382-8.